Spontaneous Electrical and Calcium Oscillations in Unstimulated Pituitary Gonadotrophs

Yue-Xian Li,* John Rinzel,* Leoncio Vergara,‡ and Stanko S. Stojilković§
*Mathematical Research Branch and ‡Laboratory of Cell Biology and Genetics, National Institute of Diabetes and Digestive and Kidney Disorders, and §Endocrinology and Reproductive Research Branch, National Institute of Child Health and Human Development, National Institutes of Health, Bethesda, Maryland 20892 USA

ABSTRACT Single pituitary cells often fire spontaneous action potentials (APs), which are believed to underlie spiking fluctuations in cytosolic calcium concentration ($[Ca^{2+}]_i$). To address how these basal $[Ca^{2+}]_i$ fluctuations depend on changes in plasma membrane voltage (V), simultaneous measurements of V and $[Ca^{2+}]_i$ were performed in rat pituitary gonadotrophs. The data show that each $[Ca^{2+}]_i$ spike is produced by the Ca^{2+} entry during a single AP. Using these and previously obtained patch-clamp data, we develop a quantitative mathematical model of this plasma membrane oscillator and the accompanying spatiotemporal $[Ca^{2+}]_i$ oscillations. The model demonstrates that AP-induced $[Ca^{2+}]_i$ spiking is prominent only in a thin shell layer neighboring the cell surface. This localized $[Ca^{2+}]_i$ spike transiently activates the Ca^{2+}-dependent K^+ current resulting in a sharp afterhyperpolarization following each voltage spike. In accord with experimental observations, the model shows that the frequency and amplitude of the voltage spikes are highly sensitive to current injection and to the blocking of the Ca^{2+}-sensitive current. Computations also predict that, leaving the membrane channels intact, the firing rate can be modified by changing the Ca^{2+} handling parameters: the Ca^{2+} diffusion rate, the Ca^{2+} buffering capacity, and the plasma membrane Ca^{2+} pump rate. Finally, the model suggests reasons that spontaneous APs were seen in some gonadotrophs but not in others. This model provides a basis for further exploring how plasma membrane electrical activity is involved in the control of cytosolic calcium level in unstimulated as well as agonist-stimulated gonadotrophs.

INTRODUCTION

Secretory cells in the anterior pituitary gland are electrically excitable. Spontaneous action potentials (APs) have been recorded in several types of normal pituitary cells, including lactotrophs (Ingram et al., 1986; Lewis et al., 1988), somatotrophs (Lewis et al., 1988), gonadotrophs (Kukuljan et al., 1992), melanotrophs (Valentijn et al., 1991), and also some pituitary cell lines (Kidokoro, 1975; Adler et al., 1983; Korn et al., 1991). The firing frequency is ~1 Hz or lower (Stojilković and Catt, 1992). In some experiments, the spontaneous firing of APs was found sensitive to both dihydropyridine (DHP) calcium channel blockers and the sodium channel blocker tetrodotoxin (TTX) (Adler et al., 1983; Biales et al., 1977), while in others only to DHP (Kidokoro, 1975; Dufy et al., 1979, Guerineau et al., 1991; Kukuljan et al., 1992). The ionic bases of voltage spiking in these cells have been extensively studied. Thus, two types of voltage-gated Ca^{2+} channels, the T-type (fast and transient) and the L-type (long-lasting and DHP-sensitive), were found in all pituitary cell types studied so far (Dubinsky and Oxford, 1984; Lewis et al., 1988; Simasko et al., 1988; Stutzin et al., 1989; Marchetti et al., 1990, Bosma and Hille, 1992; Guerineau et al., 1991; Keja and Kits, 1994). TTX-sensitive sodium channels were also found in some of the pituitary cells (Dubinski and Oxford, 1984; Marchetti et al., 1990; Mason and Skidar, 1988; Tse and Hille, 1993).

Calcium imaging and photometric experiments in unstimulated pituitary cells also revealed spiking fluctuations in cytoplasmic Ca^{2+} concentration ($[Ca^{2+}]_i$) around a basal level of 140 ~ 220 nM. These low-amplitude fluctuations were observed in gonadotrophs (Iida et al., 1991; Rawlings et al., 1991), somatotrophs (Holl et al., 1988), corticotrophs (Guerineau et al., 1991), lactotrophs (Nelson and Hinkle, 1994), and GH cell lines (Schlegel et al., 1987). The frequency fluctuates in single cell recordings and varies from cell to cell. However, clearly separated, identifiable $[Ca^{2+}]_i$ spikes were recorded only during low frequency (<1 Hz) oscillations. Each spike is characterized by a sharp upstroke followed by a long tail of slow decay. The sensitivity of these $[Ca^{2+}]_i$ fluctuations to extracellular Ca^{2+} concentration ($[Ca^{2+}]_e$) and to Ca^{2+} channel blockers indicates that these $[Ca^{2+}]_i$ oscillations are produced by Ca^{2+} entry through voltage-dependent channels on the plasma membrane (Iida et al., 1991). In accord with this, coincident measurements of membrane potential (V) and $[Ca^{2+}]_i$ in GH_3 cells showed that spontaneous firing could initiate $[Ca^{2+}]_i$ oscillations (Schlegel et al., 1987).

Because the spontaneous oscillator operates in the absence of agonist and is driven by plasma membrane electrical activity, Berridge (1990) calls it the "plasma membrane oscillator" to avoid confusing it with the cytoplasmic calcium oscillator that involves Ca^{2+} release from intracellular stores, activated by second messengers such as the inositol trisphosphate ($InsP_3$) and the cADP ribose. Plasma membrane oscillators are known to play physiologically

Received for publication 21 December 1994 and in final form 20 June 1995.

Address reprint requests to Dr. Yue-Xian Li, MRB/NIDDK, 9190 Wisconsin Ave., Suite 350, Bethesda, MD 20814-3897. Tel. 301-496-4325; Fax: 301-402-0535; E-mail: yxli@helix.nih.gov.

0006-3495/95/09/785/11 $2.00

significant roles in some pituitary endocrine cells. Ca^{2+} entry induced by AP firing was found necessary for basal hormone secretion in lactotrophs and somatotrophs (Stojilković et al., 1988) and for refilling intracellular Ca^{2+} pools after depletion caused by agonist-induced Ca^{2+} release in somatotrophs and gonadotrophs (Thorner et al., 1988; Kukuljan et al., 1994).

The present work further explores quantitatively the relation between the voltage firing and associated $[Ca^{2+}]_i$ spiking in unstimulated pituitary cells. A mechanistic biophysical model is developed and analyzed to account for the observed behaviors and to make further predictions. The cell model in our present study, the pituitary gonadotroph, is of special interest to a general understanding of Ca^{2+} signaling in pituitary cells. When stimulated by its physiological agonist, gonadotropin-releasing hormone (GnRH), transients of large amplitude $[Ca^{2+}]_i$ spikes were recorded (see review by Stojilković and Catt, 1992). Therefore, two $[Ca^{2+}]_i$ oscillators coexist and interact in gonadotrophs, a plasma membrane oscillator and a cytoplasmic oscillator (Stojilković et al., 1992; Li et al., 1994). Complete understanding of Ca^{2+} signaling in stimulated cells depends not only on the properties of the two individual oscillators when dissociated, but also on their properties when coupled (Keizer and De Young, 1993; Y. X. Li, S. S. Stojilković, J. Keizer, and J. Rinzel, manuscript in preparation).

Our plasma membrane oscillator model is described by a Hodgkin-Huxley-like set of equations (Hodgkin and Huxley, 1952) coupled to the equation for Ca^{2+} diffusion into the cell center. The gating equations for the ionic channels are based on whole-cell patch-clamp data from gonadotrophs. Here, focusing on the plasma membrane oscillator for unstimulated cells, we assume that the cytoplasm of the model cell is passive; it allows neither agonist-induced $[Ca^{2+}]_i$ oscillations nor Ca^{2+}-induced Ca^{2+} release. However, it underlies $[Ca^{2+}]_i$ homeostasis, i.e., the maintenance of a fixed calcium level. The model enables us to understand the $[Ca^{2+}]_i$ fluctuations associated with plasma membrane electrical activity, and moreover to suggest reasons why spontaneous APs were found in some gonadotrophs but not in others.

MATERIALS AND METHODS

Mathematical model

Previous experiments suggest that the plasma membrane electrical activity of gonadotrophs is determined primarily by two types of Ca^{2+} channels and two types of K^+ channels (Stutzin et al., 1989; Marcheti et al., 1990; Kukuljan et al., 1992; Tse and Hille, 1993). Using the data from these experiments, we formulate a Hodgkin-Huxley-type model, beginning with the current balance equation:

$$c_m \dot{V} = I_{app} - I_{Ca-L} - I_{Ca-T} - I_{K-DR} - I_{K-Ca} - I_L \quad (1)$$

Here, I_{Ca-L} represents the high-threshold voltage-activated, dihydropyridine-sensitive Ca^{2+} current given by $I_{Ca-L} = g_{Ca-L} m_L^2 \phi_{Ca}(V)$ where m_L is the activation gating variable and $\phi_{Ca}(V)$ is the Goldman-Hodgkin-Katz (GHK) expression (see Hille, 1984) for the driving force $\phi_{Ca}(V) = V[\bar{C}_i - \bar{C}_o \exp(-z_{Ca}FV/RT)]/[1 - \exp(-z_{Ca}FV/RT)]$, with $z_{Ca} = 2$. In ϕ_{Ca}, we replaced the time-varying $[Ca^{2+}]_i$ by a constant $\bar{C}_i$, since changes in the driving force caused by $[Ca^{2+}]_i$ variation within the physiological range have little effect on the electrical activity of the model (not shown); $\bar{C}_o$ is the extracellular Ca^{2+} concentration. I_{Ca-T} is a transient Ca^{2+} current (similar, but not identical, to the T-type current found in some neurons), written here as $I_{Ca-T} = g_{Ca-T} m_T^2 h_T \phi_{Ca}(V)$, where m_T and h_T are the activation and inactivation gating variables.

Our analysis of experimental data (E. Rojas, unpublished results) for the delayed-rectifier K^+ channel leads to the following representation: $I_{K-DR} = g_{K-DR} n \phi_K$ where activation n appears linearly, and again we use a GHK driving force. Our model also has a small leakage current, $I_L = g_L(V - V_L)$.

Each voltage-dependent gating variable q satisfies an equation of the form:

$$\dot{q} = (q_\infty - q)/\tau_q \quad (2)$$

where the equilibrium function is Boltzmann-like: $q_\infty(V) = 1/[1 + \exp(-(V - V_q)/k_q)]$ and the time constant functions for m_L and m_T satisfy $\tau_q(V) = \bar{\tau}_q \times \tau(V)$ with $\tau(V)$ defined by

$$\tau(V) = \frac{1}{\exp[(V - V_\tau)/k_\tau] + 2\exp[-2(V - V_\tau)/k_\tau]} \quad (3)$$

The time constants, τ_{hT} and τ_{nk}, are voltage independent. A sodium current has been seen in gonadotrophs (Marcheti et al., 1990; Tse and Hille, 1993) and was shown to increase the AP amplitude when the membrane was released from hyperpolarization (Tse and Hille, 1993). However, since its role in spontaneous AP firing is limited as compared with that of the Ca^{2+} currents (Kukuljan et al., 1992), we do not include it in our model.

To describe quantitatively I_{K-Ca}, the apamin-sensitive Ca^{2+}-activated K^+ current, we note that its current-voltage relation is almost linear (Kukuljan et al., 1992, 1994) and that it responds to changing $[Ca^{2+}]_i$ almost instantaneously. Thus, we use:

$$I_{K-Ca} = g_{K-Ca} \frac{C_R^{n_c}}{C_R^{n_c} + K_c^{n_c}} \phi_K \quad (4)$$

where C_R is the calcium concentration at the inner face of the plasma membrane.

The available experimental voltage-clamp data, as cited above, were used to obtain values for the biophysical parameters for the voltage-gated ionic currents of our model (see Table 1). Peak and/or steady-state $I - V$ relations were calculated for these currents (peak values of Ca^{2+} currents were obtained for step increases in V from a holding value of -80 mV). From these $I - V$ curves (not shown) we estimated the magnitudes of these currents. Thus, the maximum peak Ca^{2+} current can reach 250 pA. The outward I_{K-DR} can reach 280 pA for $V = 0$ mV. For V between -40 and 0 mV, the $I - V$ curves for I_{K-DR} and I_{K-Ca} (at $[Ca^{2+}]_i = 1$ μM) are almost linear with slopes (i.e., conductances) of ~12 and 1.5 nS, respectively. Within the same voltage range, the maximum slopes (conductances) are roughly 7 and 12 nS in the $I - V$ curves of I_{Ca-T} (peak) and I_{Ca-L} (steady state).

We complete our formulation with a reaction-diffusion equation for calcium concentration, $C = [Ca^{2+}]_i$, in the passive cytoplasm of the model cell:

$$\frac{\partial C}{\partial t} = \tau^{-1}(C_{eq} - C) + D\nabla^2 C \qquad \text{in cell interior}$$

$$D_o \frac{\partial C}{\partial r}\bigg|_{r=R} = j_{pm} \equiv -\alpha[I_{Ca-T} + I_{Ca-L}] - j_{pump} \quad (5)$$

at cell surface

TABLE 1 Parameter values of the plasma membrane model

Parameter	Model value	Experimental value	Source/reference
d_{cell} (cell diameter)	20 μm	15 ~ 25 μm	This paper
V_{cell} (cell volume)	4.2 pL		$\pi d_{cell}^3/6$
A_{cell} (cell surface area)	1250 μm^2		πd_{cell}^2
c_m (cell surface capacity)	12.5 pF		$[1(\mu F/cm^2)]A_{cell}$
$f([Ca^{2+}]_{cyt}^{free}/[Ca^{2+}]_{cyt}^{total})$	0.01	0.01	Neher and Augustine (1992), Tse et al. (1994)
V_{cell}^e (V_{cell}/f)	420 pL		V_{cell}/f
$\alpha(1/2FA_{cell})$	4.144(μM · μm/s · pA)		$1/(2F\,A_{cell})$
$\beta(A_{cell}/V_{cell})$	0.3 μm		A_{cell}/V_{cell}
F_{RT} ($F/(RT)$)	0.0375 mV^{-1}		$F/(RT)$
$\bar{C}_o$, $\bar{C}_i$	2.5, $2 \cdot 10^{-4}$ mM	2.5, $2 \cdot 10^{-4}$ mM	Kukuljan et al. (1992, 1994)
$\bar{K}_o$, $\bar{K}_i$	5, 140 mM	5, 140 mM	Kukuljan et al. (1992, 1994)
g_{Ca-L}	6.8 nS/mM	6.2 nS/mM	Stutzin et al. (1989)
g_{Ca-T}	7.5 nS/mM	6.8 nS/mM	Stutzin et al. (1989)
g_{K-DR}	0.1 nS/mM	0.12 nS/mM	*
g_{K-Ca}, K_c, n_c	0.06 nS/mM, 0.6 μM, 4		Kukuljan et al. (1992)
g_l	0.02 nS		
V_{ml}, k_{ml}	−12, 12 mV	−12, 13 mV	Stutzin et al. (1989)
V_{mt}, k_{mt}	−30, 9 mV	−30, 9 mV	Stutzin et al. (1989)
V_{mh}, k_{mh}	−50, 4 mV	−43, 7 mV	Stutzin et al. (1989)
V_{nk}, k_{nk}	−5.1, 12.5 mV	−5.1, 12.5 mV	*
V_τ, k_τ	−60, 22 mV	−60, 22 mV	*
V_l	−55 mV		
$\bar{\tau}_{ml}$	30 ms	30 ms	*
$\bar{\tau}_{mt}$	10 ms	10 ms	*
τ_{ht}	15 ms	15 ms	*
τ_{nk}	22.5 ms	22.5 ms	*
v_p, K_p, n_p	12(μM · μm/s), 0.1 μM, 2		
D, D_0	20, 800 $\mu m^2 \cdot s^{-1}$	15, 300 $\mu m^2 \cdot s^{-1}$	Allbritton et al. (1992)
τ	0.5 s		
C_{eq}	0.1 μM		

Parameter values in our model and the corresponding experimental values. Most channel parameters acquire values directly measured in experiments. For each experimental value provided here, the reference source is cited (in right column). Notice that * stands for (unpublished) parameter values obtained in analyzing the whole-cell patch-clamp data provided by Dr. Eduardo Rojas and his colleagues. Since the GHK driving force ($\phi(V)$ with a unit of mV · mM) is used in our model, all effective conductances (except g_l) bear a unit of nS/mM.

where ∇^2 is the Laplacian operator in spherical coordinates, r is the distance from the center of the spherical cell, and the R is the radius of the cell. For all simulations here we assume that C has a spherically symmetric profile, $C = C(r, t)$. The only nonlinearity appears in the boundary condition at the cell surface. D and D_o are respectively the Ca^{2+} diffusion coefficients in buffered and buffer-free cytoplasmic media (Alibritton et al., 1992), and experimental estimates of the values of τ, D, and D_o have been achieved (see Table 1). We use D_o in the boundary condition because calcium enters the cell unbound. The net calcium flux across the membranes is the difference between inward flux through the calcium channels and outward Ca^{2+} extrusion by the Ca^{2+} pump, j_{pump}, where

$$j_{pump} = v_p \frac{C_R^{n_p}}{C_R^{n_p} + K_p^{n_p}} \tag{6}$$

Again, C_R is the Ca^{2+} concentration at the inner face of the plasma membrane. α involves Faraday's constant and the cell surface area, v_p is the maximum flux density of the pump. The passive cytoplasm is characterized by a time constant τ for restoring C to its equilibrium level C_{eq} by intracellular Ca^{2+} pools.

For numerical simulations, we introduce a new variable $U = r(C - C_{eq})$ and obtain a simpler diffusion problem (Crank, 1975):

$$\begin{aligned} &\frac{\partial U}{\partial t} = -\frac{U}{\tau} + D\frac{\partial^2 U}{\partial r^2} && \text{in cell interior} \\ &U(0, t) = 0 && \text{at cell center} \\ &\left.\frac{\partial U}{\partial r}\right|_{r=R} = \frac{R j_{pm}(t)}{D_0} + \frac{U(R, t)}{R} && \text{at cell surface} \end{aligned} \tag{7}$$

where the boundary condition at the cell center is determined by the definition of $U(r, t)$. Therefore, the calcium distribution is determined from $C(r, t) - C_{eq} = U(r, t)/r$, and with special consideration at $r = 0$, using l'Hopital's rule, we have $C(0, t) - C_{eq} = \partial U/\partial r|_{r=0}$.

Numerical methods

The ordinary differential equations (ode) for a reduced model with a lumped cytoplsam (see Results) were integrated using Gear's method with

error tolerance parameter equal to 10^{-9}. Bifurcation diagrams of ode solutions (see Fig. 3 *C*) were computed using AUTO (Doedel, 1981) as incorporated in Bard Ermentrout's program XP-PAUT (email: bard@mthbard.math.pitt.edu). The partial differential equation (pde) of our full model was discretized and solved with the Crank-N-colson method with $\delta r = 0.05$ μm and $\delta t = 0.1$ ms. This parameter choice guarantees satisfactory accuracy and convergence, as tested by comparison with the analytical solution for fixed Ca^{2+} influx at the plasma membrane. Periodic solutions for the bifurcation diagram of the pde (see Fig. 8) were obtained by numerically integrating the equations, allowing transients to die out. Steady states can be obtained analytically (see Appendix).

Experimental procedures

Gonadotrophs were prepared by enzymatic dispersion of anterior pituitary glands obtained from ovariectomized rats as described in Stojilkovic et al., 1992. Cells were incubated in median 199 at 37°C in 5% CO_2, 95% air, and used in electrophysiological and $[Ca^{2+}]_i$ measurements 48–72 h after plating. Cells were placed on the stage of an inverted microscope and membrane potential was measured under current clamp conditions using the nystatin-perforated patch clamp technique. Extracellular medium for recording consisted of (in mM) 141 NaCl, 5 KCl, 2.6 $CaCl_2$, 1 $MgCl_2$, 10 Na-HEPES (pH = 7.35), and 5 glucose. Electrodes were pulled from soft capillary glass (2 ~ 4 MΩ) and filled with a solution containing (in mM): 120 K aspartate, 20 KCl, 10 HEPES, and 3 $MgCl_2$ (pH = 7.15 with NaOH). Nystatin (Sigma Chemical Co., St. Louis, MO) was added from a stock solution in dimethylsulfoxide to obtain a final concentration of 100 ~ 200 μg/ml. Membrane potential measurements were carried out using an EPC-7 patch amplifier (List-Electronics, Darmstadt-Eberstadt, Germany). Liquid junction potentials were compensated before starting each experiment.

For simultaneous recording of V and $[Ca^{2+}]_i$, cells plated on glass coverslip were incubated for 45 ~ 60 min in a loading solution containing Indo-1 AM (2 μM) and pluronic acid (0.02%) of the following composition (in mM): 141 NaCl, 5 KCl, 2.6 $CaCl_2$, 1 $MgCl_2$, 10 Na-HEPES, 5 $NaHCO_3$, and 5 D-glucose, pH = 7.4. Cells were placed on the stage of an inverted microscope provided with two splitter-filter cassettes. One beam splitter was used to send the excitation light (350 ± 10 nm) to the cells and the fluorescent light emitted by Indo-1 acid within the cells (>400 nm) to the second cassette. The second dichroic mirror was used to split the fluorescent light into beams of light centered at 410 and 485 nm (±5 nm), respectively. The intensity of the light at each wavelength was continously measured using a photomultiplier.

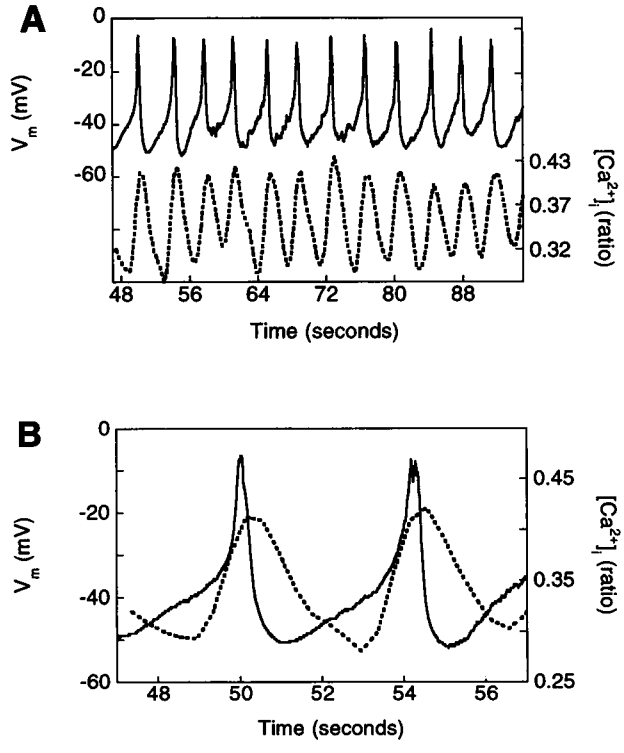

FIGURE 1 Simultaneous recording of membrane voltage V and $[Ca^{2+}]_i$ during spontaneous firing of APs in a single identified gonadotroph. $[Ca^{2+}]_i$ was monitored with the fluorescent probe Indo-1 during electrophysiological recordings obtained with the patch clamp technique in nystatin-perforated whole cell configuration (see Experimental Procedures). $[Ca^{2+}]_i$ measurement covers the whole cytoplasmic volume. The voltage profile and frequency did not differ from those observed in Indo-free cells indicating that the dye-loading did not affect the plasma membrane oscillator. Here, AP occurred spontaneously without any stimulation. The cell was identified as a gonadotroph by showing typical GnRH-induced responses when GnRH was applied at the end of the experiment. (*A*) Time courses of V (*top*, ——) and $[Ca^{2+}]_i$ (*bottom*, ·····). The calculated $[Ca^{2+}]_i$ amplitude was about 100 nM above the basal. (*B*) Profiles of two action potentials and the coincident $[Ca^{2+}]_i$ fluctuations are plotted with an extended time scale.

RESULTS

Calcium oscillations due to spontaneous action potentials

Spontaneous voltage firing in gonadotrophs is associated with marked changes in $[Ca^{2+}]_i$. Fig. 1 *A* shows a simultaneous record of the membrane potential V and $[Ca^{2+}]_i$ in a single identified gonadotroph. $[Ca^{2+}]_i$ increases concomitantly with V to a maximum of ~100 nM above the basal. The enlarged time course of two APs and the accompanying $[Ca^{2+}]_i$ spikes in Fig. 1 *B* clearly demonstrate the one-to-one correspondence of the voltage and the $[Ca^{2+}]_i$ spikes previously recorded in separate electrophysiological and calcium measurements. V slowly ramps up before reaching a spiking threshold and sharply hyperpolarizes after the spike. The voltage spike causes a rapid $[Ca^{2+}]_i$ upstroke, while the slow decay of $[Ca^{2+}]_i$ between spikes mirrors the slow up-ramp of V.

In the majority of cells observed (~70%) the AP spike does not overshoot 0 mV (Fig. 1). In other cells, however, an AP can reach +5 to +15 mV (Fig. 2 *B*). Each AP can be thought of as having two phases, the (depolarizing) spike phase and the (hyperpolarized) interspike phase. Comparing APs recorded from different cells (Fig. 2 *A*), little difference was found among spikes except in the peak amplitude. However, the slope and duration of the ramping depolarization in the interspike phase varied considerably. Therefore, AP frequency often changes in a given cell (stochastically and/or slowly drifting) and from cell to cell. The frequency is very sensitive to current injections. A small depolarizing current (1 pA) can significantly accelerate the AP firing (Fig. 2 *B*), and hyperpolarizing current injections of similar magnitude eliminate the APs (not shown). The frequency rarely exceeded 2 Hz but could be as low as 0.1 Hz; 1 Hz was typical. However, good quality records of simultaneously measured membrane potential and cystosolic cal-

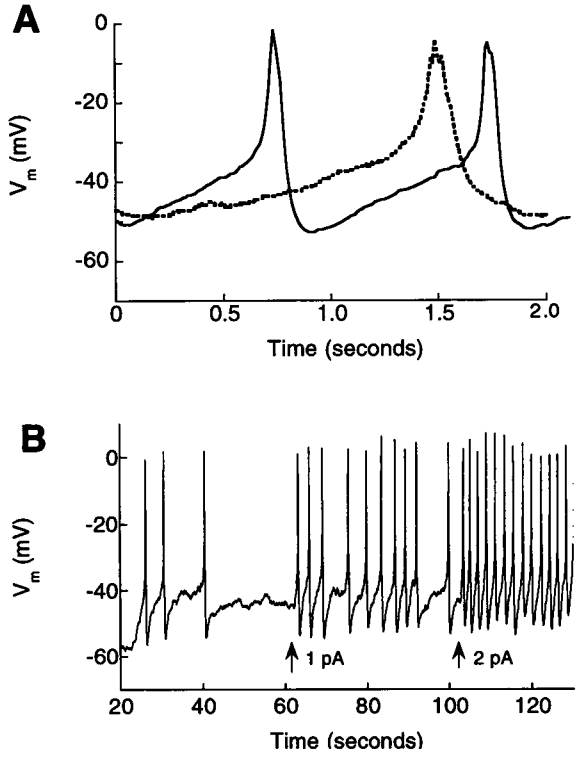

FIGURE 2 Characterization of APs in single pituitary gonadotrophs. (*A*) Volgate time course of spontaneous AP firing recorded from two isolated cells. One cell fires with the typical frequency of 1 Hz (——); the other fires at about 0.5 Hz (·····). Only one period out of a train of repetitive APs is plotted for the dotted trace. (*B*) Sensitivity of the firing frequency to current injection is demonstrated by two step increases in I_{app}.

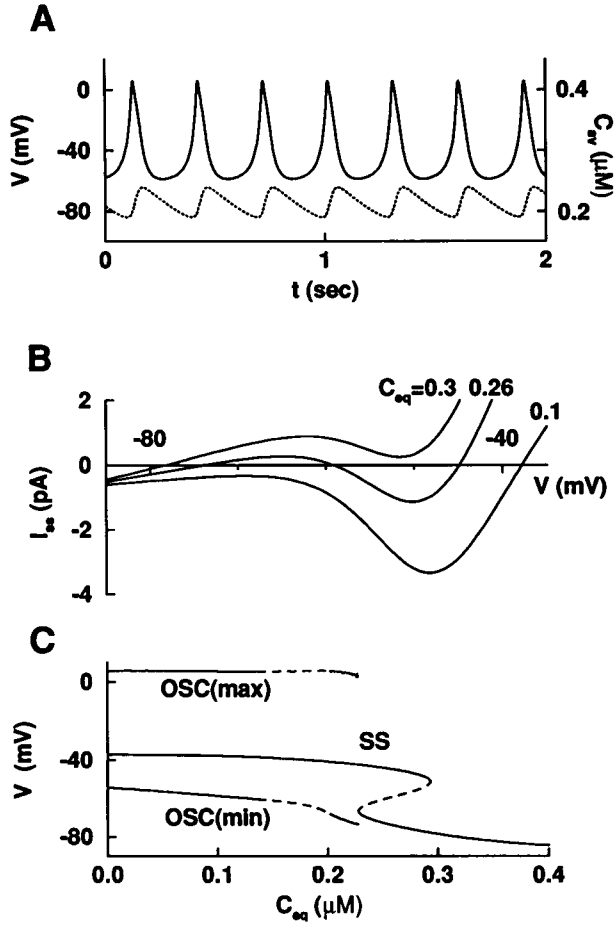

FIGURE 3 The plasma membrane oscillator with lumped cytoplasm described by Eqs. 1–4, 8. (*A*) Time course of plasma membrane voltage V (——) and the spatially averaged cytoplasmic calcium concentration C_{av} (·····). Notice the high frequency (>3 Hz) and the absence of afterhyperpolarization in V. (*B*) Total current at equilibrium, I_{ss}, for V clamped at values between −80 and −40 mV. Zones of I_{ss} correspond to steady states of the model. When C_{eq} is high (e.g., 0.3 μM), V rests at around −80 *mV*; when C_{eq} is low (0.1 μ*M*), it stays at about −40 *mV*. For intermediate C_{eq} values (e.g., 0.26 μM), the I_{ss} curve has three zero-crossings, corresponding to three possible steady states of V; two are stable (bistability), and the middle one is unstable. (*C*) Overall behavior as a function of C_{eq} in a bifurcation diagram. Steady state value of V as a function of C_{eq} is labeled SS. Maximum and minimum of V during tonic AP spiking are also plotted against C_{eq} (labeled OSC). The unstable states (not complete here) are plotted (- - - -). Standard parameter values in Table 1 were used.

cium (Fig. 1) were generally obtained only for low frequency oscillations.

The lumped cytoplasm approximation

In models for intracellular calcium handling one frequently treats calcium as time-varying but spatially uniform in a specified region of the cytoplasmic volume, adjacent to the plasma membrane. For a small cell, this region might be the entire cytoplasmic volume of the cell. This is equivalent to assuming a large diffusion coefficient.

To gain more insight into the effects of diffusion, we briefly consider this limiting situation. Our calcium transport equation and boundary condition are now replaced by:

$$\dot{C}_{av} = (C_{eq} - C_{av})/\tau + f\beta j_{pm} \qquad (8)$$

where j_{pm}, defined in Eq. 5, is the net Ca^{2+} flux through the plasma membrane; f is the Ca^{2+} buffering factor of the cytoplasm (Neher and Augustine, 1992; Tse et al., 1994; Wagner and Keizer, 1994); β is the surface-to-volume ratio (see Table 1).

This lumped cytoplasm model shows spontaneous firing of APs when C_{eq} is not too large (Fig. 3 *A*). However, as compared with experimentally measured profiles (Fig. 1), the frequency is too high and the V variation is almost sinusoidal in contrast to the sharp afterhyperpolarization (the vertical downstroke in V immediately after the peak in Fig. 1). Because of the rapid transport of Ca^{2+} away from the plasma membrane in this models, the effects of calcium on the hyperpolarizing current I_{K-Ca} and the electrical activity are underestimated.

In addition to the spontaneous oscillatory activity, this reduced model also shows the coexistence of a stable resting state with the oscillatory state. This resting state corresponds to a zero-crossing of the steady-state current-voltage relation, $I_{ss} - V$. The combined action of the four currents in the model results in an N-shaped $I_{ss} - V$ curve (Fig. 3 *B*).

If C_{eq} is large, I_{ss} is mostly outward having a single zero crossing with $V \approx V_K$; the rest state is hyperpolarized. At lower levels of C_{eq}, the rest level is around −40 mV. In an intermediate range, there is bistability. The dependence of these steady potential levels on C_{eq} is summarized in the bifurcation diagram of Fig. 3 *C*. The autorhythmic state is also represented here, by the two nearly horizontal curves (labeled OSC) for the maximum and minimum V values during the spontaneous membrane oscillations. The basic structure of this diagram is also found for the full model (described below), including bistability, in certain parameter regimes.

Action potentials and spatiotemporal oscillations of $[Ca^{2+}]_i$

To overcome the shortcomings of the lumped model, we now study the full model (Eqs. 1–5) and thereby take into account the localized distribution of Ca^{2+} that enters through voltage-gated calcium channels. We do not, however, represent the extremely high localization of Ca^{2+} at the mouth of an open Ca^{2+} channel. While $[Ca^{2+}]_i$ can reach hundreds of μM in such domains, these localized peaks are physiologically relevant only for co-localized processes with time scales faster than that of Ca^{2+} binding to its buffers (Llinás et al., 1992; Roberts, 1994). In our case, we do not suspect such co-localization, and the time scales of interest are slower than those for buffering and for the lateral spread and spatial averaging of Ca^{2+} in a layer neighboring the plasma membrane. Thus we consider only radial diffusion, and expect that the laterally equilibrated $[Ca^{2+}]_i$ might reach at most 1 μM after a depolarizing voltage pulse (Hernández-Cruz et al., 1990; Sala and Hernández-Cruz, 1990).

Fig. 4 shows the time courses of membrane potential V and $[Ca^{2+}]_i$ computed with our full model. The theoretical calcium time course in Fig. 4 *A* represents the instantaneous, spatially averaged $[Ca^{2+}]_i$, $C_{av}(t)$; it corresponds to the calcium measurement in experiments. The computed profiles in Fig. 4 *A* agree well (in amplitudes, shapes, and phasic relationships) with the experimentally observed ones (Fig. 1 *B*), as selected from slower cells that allow simultaneous measurement of V and $[Ca^{2+}]_i$ (Kukuljan et al., 1992; Stojilković et al., 1992). The simulated spikes have frequency closer to those of typical experiments in which voltage only is recorded. Moreover, in contrast to results with a lumped cytoplasm model, the computed voltage shows the sharp afterhyperpolarization typical of the observed APs (Fig. 1). This is because $[Ca^{2+}]_i$, highly elevated near the plasma membrane, strongly and promptly activates the outward current I_{K-Ca}. The computed C_{av} time course shows a sharp rise and slow fall, as does the experimental record (Iida et al., 1991, and Fig. 1 *B*). Here again, in contrast to Fig. 3, the sharp rise reflects the localization of Ca^{2+}. Examining the temporal relationship between V and C_{av} we see that C_{av} starts increasing when V exceeds −50 mV (where the Ca^{2+} currents activate); C_{av} peaks only 12 ms after V peaks. The rapid upstroke of C_{av} follows closely the spiking of V and occurs when V starts a sharp downstroke, while the slow decay of C_{av} between spikes appears to mirror the slow up-ramp of V.

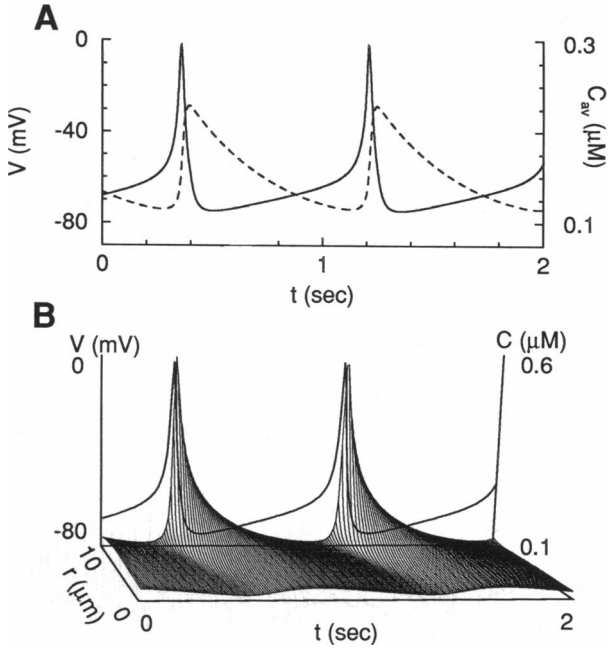

FIGURE 4 (*A*) Time course of V (——) and the spatially averaged cytoplasmic calcium concentration C_{av} (- - - -) predicted by the full diffusion model governed by Eqs. 1–4 and 5. (*B*) 3D representation of the spatiotemporal oscillations of $C(r,t)$ (*shaded surface*) during repetitive voltage firing computed with the model. The horizontal axis is time; the vertical axis on the right specifies the scale for $C(r,t)$. The accompanying variation in V is plotted as the thick solid curve on the $V - t$ plane, with the left vertical axis for its scale. The direction pointing out of the paper is the spatial variable r denoting the distance from the cell's center ($r = 0$). The amplitude of C oscillations neighboring the plasma membrane ($r = 10$ μm) exceeds 0.5 μM, while it is negligible at the center. Parameter values in Table 1 were used.

The complete spatio-temporal profile of $C(r, t)$ during an AP can be seen as the shaded surface in the 3D plot of Fig. 4 *B*. The temporal profile of the AP (Fig. 4 *B*, *thick curve*) is also projected onto the plane, $r = R = 10$ μm, where the plasma membrane is located. We notice first that Ca^{2+} is highly localized near the cell surface, agreeing well with the idea that Ca^{2+} is a local cytoplasmic messenger with an action range of ~5 μm (Allbritton et al., 1992). At locations more than 5 μm from the plasma membrane, $C(r, t)$ is little affected by the AP-induced Ca^{2+} entry. At the center of the cell, $C(0, t)$ hardly changes. Note also that, at the plasma membrane, C_R varies as rapidly as the membrane potential V.

In Fig. 5, we further identify factors that contribute to the dynamic profiles of C and V. The individual ionic currents and the plasma membrane Ca^{2+} fluxes during the depolarized phase of an AP are plotted in Fig. 5, *B* and *C*, allowing comparison of their relative amplitudes and temporal rela-

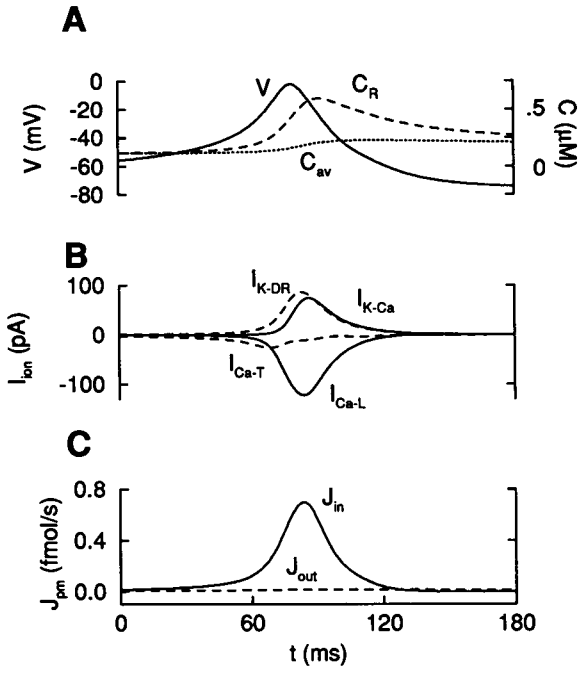

FIGURE 5 (*A*) Simultaneous plots of plasma membrane voltage V (——), calcium concentration at the plasma membrane C_R (- - - -), and the spatial average of Ca^{2+} concentration C_{av} (·····) to show their phase relationships. C_R peaks about 10 ms after V peaks. (*B*) Individual currents through plasma membrane ionic channels. The tiny leak current I_L, which varies between $-0.5 \sim 1$ pA, is not shown. The two inward (negative) currents are I_{Ca-T} (- - - -) and I_{Ca-L} (——); the two outward currents are I_{K-DR} (- - - -) and I_{K-Ca} (——). (*C*) Total inward (J_{in}, ——) and outward (J_{out}, - - - -) Ca^{2+} fluxes across the plasma membrane during the voltage spike phase of a cycle. J_{in} is due to voltage-gated Ca^{2+} channels, and J_{out} is determined by the plasma membrane Ca^{2+} pump activity. Parameter values are as in Fig. 4.

tionships. The membrane-localized $[Ca^{2+}]_i$ (C_R) fluctuation amplitude is about five times that of the spatially averaged concentration (Fig. 5 *A*). However, during part of the hyperpolarization phase of the cycle before the AP, C_R is actually lower than C_{av}. At such times, diffusion is carrying Ca^{2+} from the interior toward the membrane, where active Ca^{2+} pumping acts as a sink. In the wake of the AP, the slow decay of C_R means that I_{K-Ca} slowly deactivates, thereby accounting for the gradual rise of V toward the threshold for the next autoregenerative spike.

The voltage-gated ionic currents are substantial during the brief depolarized phase (Fig. 5 *B*), but otherwise are quite small. The leak current, always <1 pA, is outward during the spike and inward during the afterhyperpolarization between spikes (not shown). The transient Ca^{2+} current I_{Ca-T} helps initiate the AP upstroke but then largely inactivates even before I_{Ca-L} peaks. Notice that C_R begins to decrease while the membrane is still depolarized and I_{Ca-L} is still providing Ca^{2+} influx. This decrease reflects the diffusive transport of Ca^{2+} away from the membrane. The K^+ currents and I_{Ca-L} peak at about the same time. The sum of the outward currents exceeds I_{Ca-L}, thereby underlying the repolarization of the membrane.

During the afterhyperpolarization between two spikes, all the currents are <0.5 pA. In the first half of the interspike interval, I_{K-Ca} is significantly higher than the Ca^{2+} currents and I_{K-DR}. It is approximately balanced by the leak current, inward during the interval. This approximate balance means that V shows pseudo-steady state behavior, but the membrane slowly depolarizes as C_R slowly decays. Later in the interspike interval, I_{K-DR}, I_{Ca-T}, and I_{Ca-L} join the balance, as they begin to increase slowly. As the depolarization continues, V eventually reaches threshold; the balance is lost and the inward currents rise rapidly to initiate the next spike.

Fig. 5 *C* shows the corresponding calcium fluxes during a fraction of one oscillation cycle centered at the voltage peak. J_{in} (peak value, 0.697 fmol/s) is much larger than J_{out} (0.0146 fmol/s) during this phase. During the rest of the cycle, J_{out} dominates. The length of the interspike interval determines whether the net flux is inward or outward. For the parameter values used in Fig. 5, about 3/8 of the Ca^{2+} that enters the cell is extruded in each cycle. In a more complete model, which considers a much longer time scale to treat the dynamic establishment of homeostasis, C_{eq} and firing frequency would be slowly changing. The situation shown here would correspond to a phase of slowly loading the intracellular Ca^{2+} pools. With such loading, C_{eq} would increase because of higher passive leak out of the pool(s) and spiking would decrease in frequency and maybe even terminate. Such slow changes would then tend toward balancing entry with extrusion to achieve true homeostasis in unstimulated cells.

Dependence of spontaneous activity on physiological parameters

The subtle balance of currents during the interspike interval makes the oscillator extremely sensitive to current injections. Model simulations in Fig. 6 *A* show that a tiny hyperpolarizing current injection can eliminate spontaneous APs, and depolarizing current strongly accelerates the oscillations. This predicted sensitivity to current injection is consistent with the corresponding experiments shown in Fig. 2 and with the observed variability in the duration of interspike intervals within a given cell and from cell to cell.

As we have noted, the Ca^{2+}-dependent current, I_{K-Ca}, controls the length of the interspike interval. Indeed, the oscillation frequency of the model increases dramatically if this current is reduced. Fig. 6 *B* shows that the calculated frequency increases about five times when the conductance g_{K-Ca} is decreased to zero. As one expects, the afterhyperpolarization is completely eliminated. When g_{K-Ca} is increased by a factor to of two (in Fig. 6 *B* at $t = 19$ s), the amplitude decreases and complex oscillations occur. When g_{K-Ca} is very large, simple oscillations reappear but with small amplitude (V varies between -70 and -40 mV).

The slow tail of C_R and the slow dynamics of $C(r, t)$ at sites more distant from the membrane result from the slow rate of j_{pump}, the limited speed of buffered Ca^{2+} diffusion,

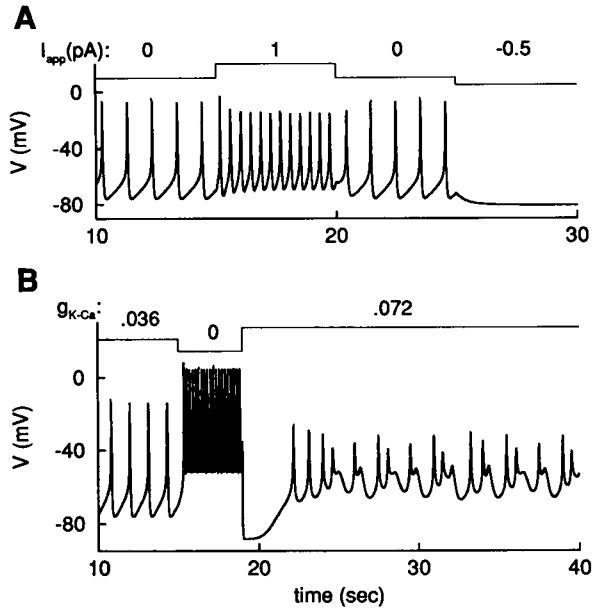

FIGURE 6 Sensitivity of spontaneous APs to current injection and to block of the Ca^{2+}-dependent current demonstrated by model simulation. (*A*) A depolarizing current of 1 pA increases the frequency significantly, while a tiny hyperpolarizing current abolishes spontaneous AP firing. (*B*) Eliminating the Ca^{2+}-dependent current does not stop the oscillation but strongly increases the frequency and eliminates the afterhyperpolarization. Enhanced g_{K-Ca} can result in complex oscillations. Notice the different time scales in (*A*) and (*B*). Parameter values are as in Fig. 4 except that in (*B*), τ = 1 s, C_{eq} = 0.15 μM, v_p = 15 μM · μm/s, D, D_0 = 15, 600 $\mu m^2/s$.

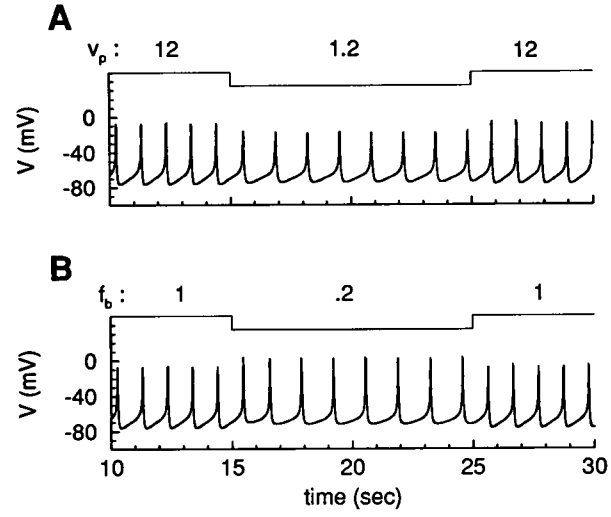

FIGURE 7 Changes in the frequency and time course of V as a function of Ca^{2+} handling parameters. (*A*) Reducing the PM Ca^{2+} pump rate slightly slows the oscillation. (*B*) Increased Ca^{2+} buffering changes the AP profile. The effect of increased buffering is modeled by decreasing D and $1/\tau$ by the factor f_b, here from 1 to 0.2. Parameter values are as in Fig 4.

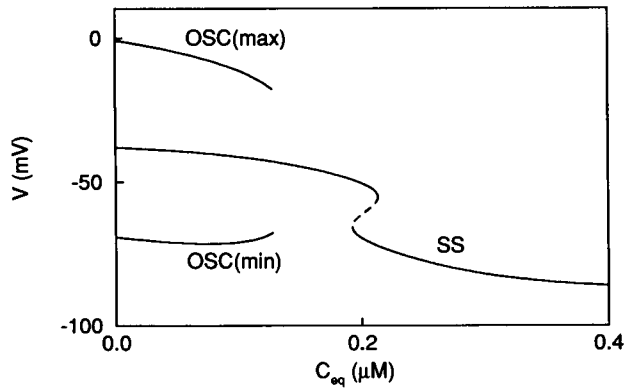

FIGURE 8 Overall behavior of the full diffusion model as a function of C_{eq} in a bifurcation diagram. Steady state value of V is plotted against C_{eq} (labeled SS). Maximum and minimum of oscillatory V states are labeled OSC. Here, as in Fig. 3 *C* for the lumped model, we find bistable behaviors between steady states and oscillations. The unstable states are shown dashed. Parameter values are as in Fig. 4, except that τ = 0.2 s, and D, D_0 = 15, 600 $\mu m^2 \cdot s^{-1}$, respectively.

and the slow time constant of Ca^{2+} homeostasis in the cell. The oscillation frequency is sensitive to the parameter values that describe these calcium-handling processes. Fig. 7 *A* shows that decreasing the plasma membrane Ca^{2+}-ATPase rate slows the oscillation. Fig. 7 *B* demonstrates that the AP firing rate drops significantly when the Ca^{2+} buffering capacity is increased, modeled here by decreasing D and $1/\tau$ by the same the factor f_b. In either case, the peak amplitude only changes slightly for most of the parameter ranges where oscillations occur. There are two effects of increasing the (immobile) Ca^{2+} buffer. It reduces the diffusion coefficient and facilitates Ca^{2+} localization, which should slow the oscillation. On the other hand, buffer sequestration of Ca^{2+} tends to reduce $[Ca^{2+}]_i$ locally. The former effect is dominant for the immobile buffer. This result has implications for the buffering effects of some mobile fluorescent dyes. They can increase Ca^{2+} diffusion rate and also enhance Ca^{2+} sequestration, thereby increasing the frequency.

Here, as in our lumped cytoplasmic model (cf Fig. 3 *C*), the homeostatic parameter C_{eq} plays an important role (cf. Fig. 8). For large C_{eq} the cell is hyperpolarized, and for smaller C_{eq} it exhibits a stable membrane potential around −40 mV. The full model also shows two types of bistablity: coexistence of continuous spiking and the stable steady state at −40 mV for a lower range of C_{eq}, and coexistence of two time-independent steady states for a slightly higher range of C_{eq}.

Relevance of the model to electrically silent gonadotrophs

About 60% of the cells observed show periodic firing, while most of the remaining cells show a stable steady potential with V fixed at about −40 mV (Kukuljan et al., 1992). The diagram in Fig. 8 suggests possible differences between the active and the silent cells. Perhaps silent cells are found in their stable rest state that may coexist with the oscillatory state, or they might be tuned parametrically into the slightly higher C_{eq} range. In the first case, a brief current pulse could initiate spontaneous oscillations; this could be tested experimentally for such cells. Our model allows an alternate

explanation for some cells being silent. Under different parameter conditions (e.g., with a larger conductance for I_{K-DR} or a smaller conductance for I_{Ca-L}) the model cell does not fire spontaneously for any value of C_{eq}, i.e., the periodic states (i.e., OSC-labeled in Fig. 8) no longer exist.

This latter situation may correspond to the case of silent, unstimulated gonadotrophs (Tse and Hille, 1992, 1993) that can be induced to fire repetitively when Bay K8644, an agonist of the L-type Ca^{2+} channel, is applied (Rawlings et al., 1991). Fig. 9 illustrates this possibility for a model cell that is spontaneously silent because its density of L-type Ca^{2+} channels is lower than that in the spontaneously active model cells; the cell rests stably at a voltage close to −40 mV. After a brief hyperpolarizing current injection (Fig. 9, *left arrow*), the cell recovers the −40 mV value in a damped oscillatory manner. This damping is consistent with V time courses seen when Ca^{2+} oscillations are induced by GnRH in electrically silent gonadotrophs (Tse and Hille, 1992, Fig. 1 *B*; 1993, Fig. 2). Model computations also indicate that, when the L-type Ca^{2+} channel conductance is increased in such cells, (e.g., in the presence of Bay K8644), the same hyperpolarizing current injection (Fig. 9, *right arrow*) switches the cell into a tonic spiking state. These results suggest that a slight underexpression (overexpression) of channels carrying an inward (outward) current is a possible reason why >30% of the unstimulated cells are electrically silent under the same culture conditions and why unstimulated cells are found active in one laboratory (Kukuljan et al., 1992) but not in others (Rawlings et al., 1991; Tse and Hille, 1992). However, different experimental techniques or other differences not related to channel expression can also render a cell electrically silent.

DISCUSSION

Most pituitary gland cells are electrically excitable, and voltage-gated calcium channels are crucial for such excitability (Ozawa and Sand, 1986). The spontaneous action potential firing in these cells is associated with the small amplitude and extracellular Ca^{2+}-dependent fluctuations in $[Ca^{2+}]_i$ (Schlegel et al., 1987; Iida et al., 1991; Rawlings et al., 1991). Simultaneous measurements of membrane voltage and $[Ca^{2+}]_i$ have revealed that a single action potential leads to a marked $[Ca^{2+}]_i$ spike in mouse lacto-somatotroph and immortalized human corticotroph cell lines (Schlegel et al., 1987; Guerineau et al., 1991). The present data demonstrate that spontaneous action potential spiking also drives small amplitude $[Ca^{2+}]_i$ oscillations in rat pituitary gonadotrophs. We constructed a mathematical model that accounts for these oscillations. Based on recent experimental data, the model incorporates Hodgkin-Huxley-type channel gating properties and a description of the spatiotemporal distribution of $[Ca^{2+}]_i$.

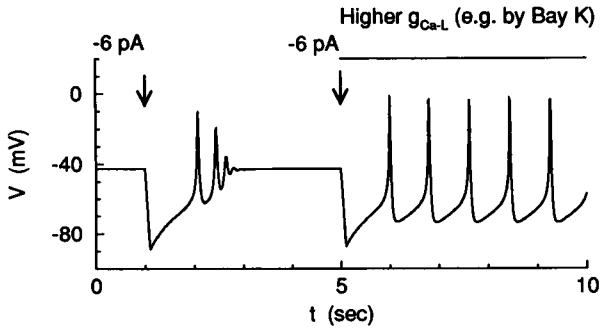

FIGURE 9 Responses of a model gonadotroph to electrophysiological stimuli. This model cell is made incapable of maintained oscillations by reducing the conductance of the normal L-type Ca^{2+} current (to 5 nS/mM). When a pulse of hyperpolarizing current (100 ms duration and 6 pA amplitude) is applied, the cell hyperpolarizes transiently and recovers to the resting voltage, −40 mV, in a damped oscillatory manner. When the L-type Ca^{2+} channel conductance is increased to 6.5 nS/mM, the resting level changes slightly but remains stable. But now, the same pulse of current injection initiates sustained oscillations. Parameter values are as in Fig. 4.

We showed that the localized distribution of Ca^{2+} after entering the cell exerts a strong influence on the frequency and temporal profile of voltage firing. The existence of Ca^{2+}-dependent K^+ channels makes the plasma membrane activity sensitive to the Ca^{2+} distribution close to the plasma membrane. On the other hand, Ca^{2+} diffuses rather slowly within the cytoplasm because of 1) the high concentration of Ca^{2+} buffers and 2) the intracellular Ca^{2+} pools that sequester or release Ca^{2+} depending on $[Ca^{2+}]_i$ level. The effective diffusion coefficient (D) for Ca^{2+} in the cytoplasm and the time scale τ for the Ca^{2+} homeostasis of the pool determines the action range of Ca^{2+} from its source: $\xi = \sqrt{D\tau}$. This value has been estimated to be about 5 μm (Allbritton et al., 1993). Therefore, we should expect significantly localized elevation of Ca^{2+} within 5 μm from its source, the plasma membrane. Accurate description of the Ca^{2+} handling of the cytoplasm becomes a necessary part of the plasma membrane model. We showed that varying parameters that influence cytoplasmic Ca^{2+} handling (parameters such as diffusion constant, buffers, pump activity) can strongly modify the frequency and temporal profile of action potential firing.

The lumped cytoplasm model is simple and straightforward but underestimates the hyperpolarizing effect of I_{K-Ca}. The full Ca^{2+} diffusion model correctly predicts Ca^{2+} localization and the associated afterhyperpolarization, but the simulation is more demanding. A compromise between the two is a coarse discretization of the cell into just two compartments. The thickness of the outer compartment is proportional to $\sqrt{D\tau}$, the Ca^{2+} action range. The two-compartment model, with properly chosen lumped transport parameters, can also reproduce dynamic behaviors of both silent and spontaneously active gonadotrophs satisfactorily (results not shown). However, the parameter values for Ca^{2+} transport between the two compartments cannot be strictly derived from a full diffusion model but can only be empirically determined.

Although the dynamic behaviors of spontaneously active and silent gonadotrophs appear quite different, the model demonstrates that they can be explained by the same biophysical mechanisms incorporated into a set of differential

equations with closely associated ranges of parameter values. A slightly lower Ca^{2+} conductance or a slightly higher K^+ conductance is sufficient to abolish spontaneous voltage firing. The model predicts that tonic firing of APs can probably occur in the silent gonadotrophs resting at the characteristic −40 mV steady state. This could be facilitated by increasing the conductance of Ca^{2+} channels or by decreasing the delayed rectifier conductance. In accord with this prediction, Rawlings et al. (1991) have reported that enhancing the L-type Ca^{2+} channel conductance by Bay K8644 causes oscillatory $[Ca^{2+}]_i$ fluctuations in silent gonadotrophs. In our experiments, the percentage of the cells showing spontaneous APs varies from preparation to preparation (from 10 to 90%). This suggests that differences in the expression of a certain channel type in cultured cells might be crucial in determining the electrical status of these cells in unstimulated conditions.

In conclusion, the present study provides a basis for understanding the relationship between AP firing and Ca^{2+} signaling in unstimulated gonadotrophs. It also yields insights into how the electrical status of gonadotrophs depends on the channel conductance and how the plasma membrane electrical activity is modulated by changes in Ca^{2+} handling parameters of the cytoplasm. Moreover, because the plasma membrane channels found in gonadotrophs are also found in other pituitary cell types, our model may have more general relevance for understanding how plasma membrane electrical activity controls Ca^{2+} entry and the basal Ca^{2+} concentration in a wider range of unstimulated pituitary cells. Because in some pituitary cell types $[Ca^{2+}]_i$ variation is crucial in controlling basal hormone secretion, the model could be used for further study of the roles of the plasma membrane oscillator in $[Ca^{2+}]_i$-secretion coupling. Of particular interest, the model allows further investigation of the coupling between the two distinct $[Ca^{2+}]_i$ oscillators, the plasma-membrane oscillator and the agonist-induced cytoplasmic oscillator.

APPENDIX

Steady-state solution of the full model

We briefly demonstrate how the steady-state solution of the full system (Eqs. 1–5) can be obtained analytically. For simplicity, we use the scaled space variable $l = r/\xi$ with $L = R/\xi$ and $\xi = \sqrt{D\tau}$. Let C_R^s represent the equilibrium value of C at the plasma membrane (i.e., when $r = R$ or $l = L$). The steady-state values of the gating variables (represented by q in Eq. 2) are trivially determined by their respective equilibrium functions ($q^\infty(V^s)$, where V^s is the equilibrium value for V). The values of V^s and C_R^s are determined by the following transcendental equations, which are obtained by letting $\dot{V} = 0$ in Eq. 1 and $\partial C/\partial t = 0$ in Eq 5 with C evaluated at the plasma membrane.

$$0 = I_{app} - I_L(V^s) - I_{Ca-L}(V^s) - I_{Ca-T}(V^s) - I_{K-DR}(V^s) - I_{K-Ca}(V^s, C_R^s) \quad (9)$$

$$C_R^s - C_{eq} = \left(\frac{R}{D_0}\right)\frac{j_{pm}(V^s, C_R^s)}{\coth(L)L - 1}$$

Where j_{pm} retains the definition in Eq. 5.

Once V^s and C_R^s are determined, $j_{pm}(V^s, C_R^s)$ will also be fixed. The steady-state calcium distribution ($C^s(l)$, $l \in [0, L]$) can thus be obtained by solving Eq. 5 with fixed $j_{pm}(V^s, C_R^s)$.

$$C^s(l) - C_{eq} = \left(\frac{R}{D_0}\right)\left(\frac{j_{pm}(V^s, C_R^s)}{\coth(L)L - 1}\right)\left(\frac{\sinh(l)L}{\sinh(L)l}\right) \quad (10)$$

Notice that Eq. 10 is identical to the second equation in Eq. 9 when $l = L$.

We are grateful to Drs. Eduardo Rojas and Manuel Kukuljan for their generosity in sharing with us their experimental data, including some unpublished data. Prof. Joel Keizer is acknowledged for helpful discussions.

REFERENCES

Adler, M., B. M. Wong, S. L. Sabol, N. Busin, M. B. Jackson, and F. F. Weight. 1983. Action potentials and membrane ion channels in clonal anterior pituitary cells. *Proc. Natl. Acad. Sci. USA.* 80:2086–2090.

Allbritton, N., T. Meyer, and L. Stryer. 1992. Range of messenger action of calcium ion and inositol 1,4,5-trisphosphate. *Science (Wash.).* 258: 1812–1815.

Berridge, M. J. 1990. Calcium oscillations. *J. Biol. Chem.* 265:9583–9586.

Biales, B., M. A. Dicher, and A. Tischler. 1977. Sodium and calcium action potential in pituitary cells. *Nature (Lond.).* 267:172–174.

Crank, J. 1975. The Mathematics of Diffusion, 2nd ed. Clarendon Press, Oxford.

Bosma, M. M., and B. Hille. 1992. Electrophysiological properties of a cell line of the gonadotrope lineage. *Endocrinology.* 130:3411–3420.

Doedel, E. 1981. A program for the automatic bifurcation analysis of autonomous systems. *Cong. Num.* 30:265–484.

Dubinsky, J. M. and G. S. Oxford. 1984. Ionic currents in two strains of rat anterior pituitary tumor cells. *J. Gen. Physiol.* 83:309–339.

Dufy, B., J. D. Vincent, H. Fleury, P. Du Pasquier, D. Gourdji, and A. Tixier-Vidal. 1979. Membrane effects of thyrotropin-releasing hormone and estrogen shown by intracellular recording from pituitary cells. *Science (Wash.).* 204:309–311.

Guerineau, N., J.-B. Corcuff, A. Tabarin, and P. Mollard. 1991. Spontaneous and corticotropin-releasing factor-induced cytosolic calcium transients in corticotrophs. *Endocrinology.* 129:409–420.

Hernández-Cruz, A., F. Sala, and P. R. Adams. 1990. Subcellular calcium transients visualized by confocal microscopy in a voltage-clamped vertebrate neuron. *Science (Wash.).* 247:858–862.

Hille, B. 1984. Ionic Channels of Excitable Membranes. Sinauer Associates, Sunderland, MA.

Hodgkin, A. L., and A. F. Huxley. 1952. A quantitative description of membrane current and its application to conduction and excitation in nerve. *J. Physiol.* 117:500–544.

Holl, R. W., M. O. Thorner, G. L. Mandell, J. A. Sullivan, Y. N. Sinha, and D. A. Leong. 1988. Spontaneous oscillations of intracellular calcium and growth hormone secretion. *J. Biol. Chem.* 263:9682–9685.

Iida, T., S. S. Stojilkovic, S. Izumi, and K. J. Catt. 1991. Spontaneous and agonist-induced calcium oscillations in pituitary gonadotrophs. *Mol. Endocrinol.* 5:949–958.

Ingram, C. D., R. J. Bicknell, and W. T. Mason. 1986. Intracellular recordings from bovine anterior pituitary cells: modulation of spontaneous activity by regulators of prolactin secretion. *Endocrinology.* 119: 2508–2515.

Keizer, J., and G. De Young. 1993. Effect of voltage-gated plasma membrane Ca^{2+} fluxes on IP_3-linked Ca^{2+} oscillations. *Cell Calcium* 14: 397–410.

Keja, J. A., and K. S. Kits. 1994. Single-channel properties of high- and low-voltage-activated calcium channels in rat pituitary melanotropic cells. *J. Neurophysiol.* 71:840–855.

Kidokoro, Y. 1975. Spontaneous calcium action potentials in a clonal pituitary cell line and their relationship to prolactin secretion. *Nature (Lond.).* 258:741–742.

Korn, S. J., A. Bolden, and R. Horn. 1991. Control of action potentials and Ca^{2+} influx by the Ca^{2+}-dependent chloride current in mouse pituitary cells. *J. Physiol. (Lond.).* 439:423–437.

Kukuljan, M., E. Rojas, K. J. Catt, and S. S. Stojilković. 1994. Membrane potential regulates inositol 1,4,5-trisphosphate-controlled cytoplasmic Ca^{2+} oscillations in pituitary gonadotrophs. *J. Biol. Chem.* 269: 4860–4865.

Kukuljan, M., S. S. Stojilković, E. Rojas, and K. J. Catt. 1992. Apamin-sensitive potassium channels mediate agonist-induced oscillations of membrane potential in pituitary gonadotrophs. *FEBS Lett.* 301:19–22.

Lewis, D. L., M. B. Goodman, P. A. St. John, and J. L. Barker. 1988. Calcium currents and fura-2 signals in fluorescence-activated cell sorted lacotrophs and somatotrophs of rat anterior pituitary. *Endocrinology.* 123:611–621.

Li, Y.-X., J. Rinzel, J. Keizer, and S. S. Stojilkovic. 1994. Calcium oscillations in pituitary gonadotrophs: comparison of experiment and theory. *Proc. Natl. Acad. Sci. USA.* 91:58–62.

Llinás, R., M. Sugimori, and R. B. Silver. 1992. Microdomains of high calcium concentration in a presynaptic terminal. *Science (Wash.).* 256: 677–679.

Marchetti, C., G. V. Childs, and A. M. Brown. 1990. Voltage-dependent calcium currents in rat gonadotrophs separated by centrifugal elutriation. *Am. J. Physiol.* 258:E589–E596.

Mason, M. T., and S. K. Skidar. 1988. Characterization of voltage-gated sodium channels in ovine gonadotrophs: relationship to hormone secretion. *J. Physiol. (Lond.).* 399:493–551.

Neher, E., and G. J. Augustine. 1992. Calcium gradients and buffers in bovine chromaffin cells. *J. Physiol. (Lond.).* 450:273–301.

Nelson, E. J., and P. M. Hinkle. 1994. Characteristics of the Ca^{2+} spike and oscillations induced by different doses of thyrotropin-releasing hormone (TRH) in individual pituitary cells and non-excitable cells transfected with TRH receptor complementary deoxyribonucleic acid. *Endocrinology.* 135:1084–1092.

Ozawa, S., and O. Sand. 1986. Electrophysiology of excitable endocrine cells. *Physiol. Rev.* 66:887–952.

Rawlings, S. R., D. J. Berry, and D. A. Leong. 1991. Evidence for localized calcium mobilization and influx in single rat gonadotropes. *J. Biol. Chem.* 266:22755–22760.

Roberts, W. M. 1994. Localization of calcium signals by a mobile calcium buffer in frog saccular hair cells. *J. Neurosci.* 14:3246–3262.

Sala, F., and A. Hernández-Cruz. 1990. Calcium diffusion modeling in a spherical neuron. Relevance of buffering properties. *Biophys. J.* 57: 313–324.

Schlegel, W., B. P. Winiger, P. Mollard, P. Vacher, F. Wuarin, G. R. Zahnd, C. B. Wollheim, and B. Dufy. 1987. Oscillations of cytosolic Ca^{2+} in pituitary cells due to action potentials. *Nature (Lond.).* 329: 719–721.

Simasko, S. M., G. A. Weiland, and R. E. Oswald. 1988. Pharmacological characterization of two calcium currents in GH3 cells. *Am. J. Physiol.* 254:E328–E336.

Stojilković, S. S., and K. J. Catt. 1992. Calcium oscillations in anterior pituitary cells. *Endocr. Rev.* 13:256–280.

Stojilković, S. S., S.-I. Izumi, and K. J. Catt. 1988. Participation of voltage-sensitive calcium channels in pituitary hormone secretion. *J. Biol. Chem.* 263:13054–13061.

Stojilković, S. S., M. Kukuljan, T. Iida, E. Rojas, and K. J. Catt. 1992. Integration of cytoplasmic calcium and membrane potential oscillations maintains calcium signaling in pituitary gonadotrophs. *Proc. Natl. Acad. Sci. USA.* 89:4081–4085.

Stutzin, A., S. S. Stojilković, K. J. Catt, and E. Rojas. 1989. Characteristics of two calcium channels in rat pituitary gonadotrophs. *Cell Physiol.* 26:C865–C874.

Thorner, M. O., R. W. Holl, and D. A. Leong. 1988. The somatotrope: an endocrine cell with functional calcium transients. *J. Exp. Biol.* 139: 169–179.

Tse, A. and B. Hille. 1992. GnRH-induced Ca^{2+} oscillations and rhythmic hyperpolarizations of pituitary gonadotropes. *Science (Wash.).* 255: 462–464.

Tse, A. and B. Hille. 1993. Role of voltage-gated Na^+ and Ca^{2+} channels in gonadotropin-releasing hormone-induced membrane potential changes in identified rat gonadotropes. *Endocrinology.* 132:1475–1481.

Tse, A., F. W. Tse, and B. Hille. 1994. Calcium homeostasis in identified rat gonadotropes. *J. Physiol. (Lond.).* 477:511–525.

Valentijn, J. A., E. Louiset, H. Vaudry, and L. Cazin. 1991. Dopamine-induced inhibition of action potentials in cultured frog pituitary melanotrophs is mediated through activation of potassium channels and inhibition of calcium and sodium channels. *Neuroscience.* 42:29–39.

Wagner, J., and J. Keizer. 1994. Effects of rapid buffers on Ca^{2+} oscillations. *Biophys. J.* 67:447–456.